

Seismic behavior evaluation of exterior beam-column joints with headed or hooked bars using nonlinear finite element analysis

S. Rajagopal^{*1}, S. Prabavathy¹ and Thomas H.-K. Kang²

¹Department of Civil Engineering, Mepco Schlenk Engineering College, Sivakasi, Tamil Nadu 626-605, India

²Department of Architecture and Architectural Engineering, Seoul National University, Gwanak-gu, Seoul 151-744, Korea

(Received November 3, 2013, Revised February 25, 2014, Accepted March 8, 2014)

Abstract. This paper studies the response of seismic behavior of reinforced concrete exterior beam-column joints under reversal loading with different anchorages and joint core details. The joint core was detailed without much confinement (group-I) and/or with proposed X-cross bars in the core (group-II). The beam longitudinal reinforcement's anchorages were designed as per ACI 352 (headed bars), ACI 318 (conventional 90° bent hooks) and IS 456 (90° bent hooks with extended tails). The nonlinear finite element analysis response of the beam-column joints was studied, along with initial and progressive cracks up to failure. The experimental and analytical results were compared and presented in this paper to make more scientific conclusions.

Keywords: reinforced concrete; exterior beam-column joint; headed bars; hooked bars; nonlinear finite element analysis; crack

1. Introduction

Structural concrete components exist in buildings in different forms. Understanding their response during different loading conditions is crucial to the development of an efficient and safe structure. Different methods have been used to study the response of structures and their structural components. Experiment-based methods are being widely used to analyze individual components and their systems under a variety of loading conditions. Experimental methods are very good in getting the response and behavior in real life condition but it is time consuming and more expensive. Thus, the use of finite element analysis (FEA) is gaining importance to analyze the structural components by simulating them with real life loading, boundary conditions and material behavior. This paper's numerical simulation is carried out with finite element software using ANSYS (2009).

Finite element analysis is a numerical one widely applied to the reinforced concrete structures based on the use of the nonlinear behavior of materials. Finite element analysis provides a tool that can simulate and predict the responses of reinforced and prestressed concrete members. A number of commercial FEA programs are available along with the advanced modules for complex

*Corresponding author, Ph.D, E-mail: srajagopals@gmail.com

analysis. FEA has been an important tool in the analysis of simple reinforced concrete (RC) components such as RC beams, columns, slabs, etc., and complex concrete structures such as offshore walls, deep beams, shear walls, beam-column joints, and FRP-strengthened structures (Xilin *et al.* 2012; Xing *et al.* 2013; Ibrahim Ary and Kang 2012; Kang *et al.* 2012). In recent years, ANSYS finite element software has been used successfully in research works to simulate the seismic behavior of reinforced concrete elements (Raongjant and Jaig 2008). Many prior researchers have developed analytical finite element models to predict the shear strength and behavior of beam-column joints (Baglin and Scott 2000; Hegger *et al.* 2004; Park and Mosalam, 2012; Shrestha *et al.* 2013; Bindhu *et al.* 2008; Bindhu and Jeya 2010; Li and Kulkarni 2010; Ayoub 2006; Al-Ta'an and Ezzadeen 1995; Kwak and Filippou 1997; Dahmani *et al.* 2010).

According to the previously conducted nonlinear finite element analyses, beam-column joints of RC frames are considered as critical regions in low-to-moderate-to-high seismic prone areas, and thus concrete quality of the critical joint region is very important. Recently the use of headed bars has become very popular for reinforcement-congested concrete structures, providing an adequate solution to reinforcing congestion problems (Chun *et al.* 2007; Kang *et al.* 2009; Kang *et al.*, 2010; Lam *et al.* 2011; Kang and Mitra 2012). For proper anchorage with joints, details of reinforcement are essential, and innovative joint designs that are capable of reducing congestion of reinforcement in the joint are desirable. Joint ASCE (American Society of Civil Engineers)-ACI (American concrete institute) Committee 352, Joints and Connections in Monolithic Concrete Structures, recommends additional research on the use of headed bars (mechanical anchorage) in designing beam-column connections of RC structures. The investigations of the beam-column connection containing longitudinal beam reinforcing bars with 90° standard bent hooks and/or mechanical anchors inside the joint core under reversal loading have been experimentally researched over the years. However, to the authors' knowledge, no sophisticated nonlinear finite element analysis has been conducted to investigate the anchorage behavior of headed bars inside a beam-column joint. Given this gap, the authors of this paper tested half-scale exterior beam-column joint specimens at MEPCO Engineering College, Sivakasi, India, and conducted research in the analytical modeling of the specimens. The joint assemblage was subjected to reversal loading using a hydraulic jack. The test results are evaluated with nonlinear finite element analysis. The analysis results are presented in this paper.

2. Nonlinear finite element analysis and elements used

Finite element analysis (FEA) involves prediction of behavior of structures with complex geometry and loads, which are very difficult to analyze. In FEA, a variety of structure types can be easily analyzed. The user just needs to know only the geometry of the structure and its boundary conditions without knowing the governing equations or the mathematics. The following presents each element's modeling schemes.

2.1 Concrete modeling

The element types for this model are shown in Table 1. The Solid65 element was used to model the concrete for the 3-D modeling of solids with or without reinforcing bars. The solid element is capable of modeling cracking in tension and crushing in compression. For example, in concrete

Table 1 Elements used in modeling

Material type	Element type in model	ANSYS element	Material model number
Concrete	Type-1	Solid65	1
Reinforcing bar	Type-2	Link180	2

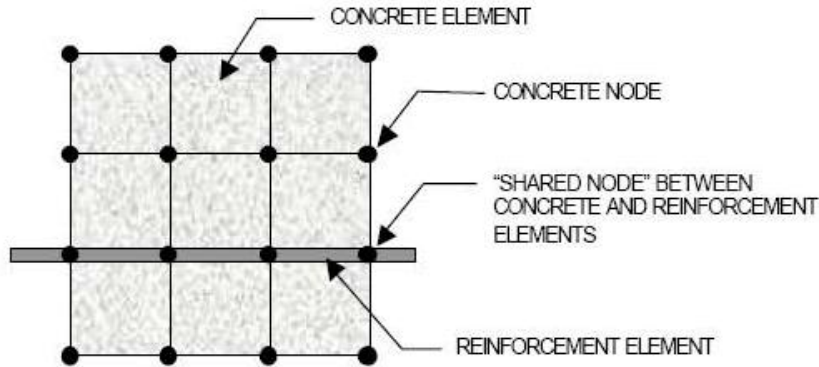


Fig. 1 Discrete method model for reinforcement in reinforced concrete (Tavarez 2001)

applications, the solid element is used to model the concrete while the reinforcing bar element is available for modeling reinforcement behavior. Other cases for which the solid element is also applicable would be reinforced composites (such as fiber-reinforced concrete) and geological materials (such as soil). The Solid65 element is defined by eight nodes having three degrees of freedom at each node: translations in the nodal x , y , and z directions.

2.2 Steel reinforcing bar modeling

The Link180 element was used to model the steel reinforcement as indicated in the Table 1. This 3-D spar element is a uniaxial tension-compression element having two nodes with three degrees of freedom and each node translations in the nodal x , y , and z directions. This element includes plasticity, creep, rotation, large deflection and large strain capabilities. The steel reinforcing bars are embedded in concrete elements (Solid65) as shown in Fig. 1 in discrete modeling. The discrete model of concrete (Solid65) and reinforcement (Link180) share the same node as shown in Fig. 1.

2.3 Element real constants

Element real constants are as shown in Table 2 that depend on the element type, which are cross-sectional properties of a beam element. For example, real constants for Beam3, the 2-D beam element, are area (AREA), moment of inertia (IZZ), height (HEIGHT), shear deflection constant (SHEARZ), initial strain (ISTRN) and added mass per unit length (ADDMAS). Not all element types require real constants, and different elements of the same type may have different real constant values.

Table 2 Real constants used in modeling

Material Type	ANSYS element	Real constant set number	Cross-sectional area (mm ²)	Diameter of rebar & Diameter of head (mm)
Concrete	Solid65	-	-	-
Reinforcing bar	Link180	1	28.3	6
Reinforcing bar	Link180	2	50.3	8
Reinforcing bar	Link180	3	113.1	12
Reinforcing bar	Link180	4	201	16
Headed bar	Link180	4	2100	35 & 60

2.4 Element material properties

The following parameters are needed to define the material model number 1 for the Solid65 elements. The element properties are indicated in Table 3 and Fig. 2. The multi-linear isotropic material uses von Mises failure criterion along with Willam and Warnke's model (1974) to define the triaxial failure of concrete type materials. The E_c is the modulus of elasticity of the concrete (EX) and ν is the Poisson's ratio (PRXY). The compressive uniaxial stress-strain values for the concrete model were obtained using the below equations with which the multi-linear isotropic stress-strain curves are obtained for the concrete (Kachlakev *et al.* 2001; Wolanski 2004; Raongjant and Jaig 2008).

$$E_c = 5000\sqrt{f'_c} \quad (1)$$

$$f = \frac{E_c \varepsilon}{1 + \left(\frac{\varepsilon}{\varepsilon_0}\right)^2} \quad (2)$$

$$\varepsilon_0 = \frac{2f'_c}{E_c} \quad (3)$$

$$E_c = \frac{f}{\varepsilon} \quad (4)$$

Where f is the stress at any strain (ε), ε is the strain at any stress (f), ε_0 is the strain at the ultimate compressive strength (f'_c) and for the multi-linear isotropic stress-strain curve, and the first point of the curve is to be defined by the user, satisfying the Hooke's law as shown in Eq. (5).

$$E = \frac{\sigma}{\varepsilon} \quad (5)$$

Where σ is the stress, ε is the strain and E is the modulus of elasticity.

Table 3 Concrete material properties for Solid65

Linear Isotropic		
E_c (EX)		26154 N/mm ²
ν (PRXY)		0.2
Density (DENS)		2400 N/mm ³
Multi-linear Isotropic		
Sl. No.	Strain	Stress (N/mm ²)
0	0.00000	0.00
1	0.00026	6.81
2	0.00060	14.78
3	0.00095	21.07
4	0.00130	25.18
5	0.00173	27.70
6	0.00213	28.30

Table 4 Concrete material constants for Solid65

1	Shear transfer coefficient for an open crack (β)	0.2
2	Shear transfer coefficients for a closed crack (β_c)	0.9
3	Uniaxial tensile cracking stress (f_r)	3.72
4	Uniaxial crushing stress (f'_c)	-28.3
5	Biaxial crushing stress	0
6	Ambient hydrostatic stress state for use with constants 7 and 8	0
7	Biaxial crushing stress (positive) under the ambient hydrostatic stress state (constant 6)	0
8	Uniaxial crushing stress (positive) under the ambient hydrostatic stress state (constant 6)	0
9	Stiffness multiplier for cracked tensile condition	0

Table 5 Reinforcement material properties for Link180

Linear Isotropic	
Elastic modulus, E_s (EX)	2.1E+05 N/mm ²
ν (PRXY)	0.3
Density (DENS)	7850 N/mm ³
Bilinear Isotropic	
Yield stress (f_y)	415 N/mm ²
Tangent modulus (E'_s)	2100 N/mm ²

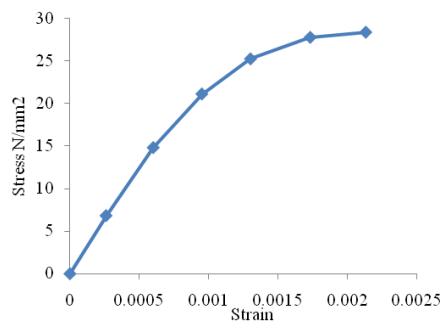


Fig. 2 Uniaxial stress-strain curve used for concrete



Fig. 3 One cycle of reversal load and load steps 1 to 4

The uniaxial stress-strain curve (Fig. 2) was built using Eqs. (1) to (3). The first point, which was defined as $0.3f'_c$ and was calculated in the linear range. The second to fifth points were calculated from Eq. (1) with ε_0 obtained from Eq. (2). The sixth point was defined at f'_c and ε_0 (0.00222), which is the crushing strain of unconfined concrete in this model.

Implementation of the Willam and Warnke material model (1974) in ANSYS requires different constants to be defined as shown in Table 3.

Typical shear transfer coefficients vary from 0 to 1, with 0 indicating a smooth crack (complete loss of shear transfer) and 1 indicating a rough crack (no loss of shear transfer). The shear transfer coefficients for open and closed cracks were determined based on the work of Kachlakev *et al.* (2001). Numerical convergence occurred when the shear transfer coefficient for an open crack dropped below the value of 0.2. No deviation of the response occurred with the change of the coefficient. Thus, the coefficient for an open crack was set to 0.2 (Table 4). The uniaxial cracking stress was based on the modulus of rupture. This value was determined using IS 456 (2000) as follows:

$$f_r = 0.70\sqrt{f'_{cu}} \quad (6)$$

where f'_{cu} is the cube concrete strength.

The uniaxial crushing stress (f_r) in this model was based on the uniaxial unconfined compressive strength. It was entered to turn off the crushing capability of the concrete element as suggested by Kachlakev *et al.* (2001). Numerical convergence has been repeated when the crushing capability was turned on.

Material model number 2 refers to the Link180 element as indicated in the Table 5. The bilinear kinematic hardening model (BKIN) was used (Kachlakev *et al.* 2001; Wolanski 2004). The bilinear model requires the yield stress (f_y) and the hardening modulus of the steel (E'_s). The constitutive law for steel behavior is as follows:

$$\sigma_s = E_s \varepsilon_s, \quad \varepsilon_s \leq \varepsilon_y \quad (7)$$

$$\sigma_s = f_y + E'_s \varepsilon_s, \quad \varepsilon_s \leq \varepsilon_y \quad (8)$$

where σ_s is the steel stress, ε_s is the steel strain, E_s is the elastic modulus of steel, E'_s is the tangent modulus of steel after yielding, $E'_s = 0.01E_s$, and f_y and ε_y are the yielding stress and strain of steel, respectively.

2.5 Analysis type

The reinforced concrete exterior beam-column joint elements are analyzed by static nonlinear finite element model under reversal loading using ANSYS (2009). Loading cycles, load applications and load steps used for the analysis are shown in Fig. 3. In the particular case considered, the analysis is of large displacement and static since this problem is performed under static nonlinear analysis.

3. Beam-column joint modeling, meshing and finite element analysis

Using the preprocessor modeling commands, nodes were generated in the outer dimension of the column specimens and similarly the nodes were created where the column reinforcing bars were located. Then the column was extruded in the y-direction as a volume up to each shear link level. Similarly the beam was extruded in the x-direction as a volume as shown in Fig. 6. All the volumes were meshed using the mesh-mapped command. After meshing, all the elements were assigned as Solid65 for concrete and each node were connected with Link180 elements for reinforcing bars as shown in Figs. 1 and 4. The overall beam-column assembly and reinforcement were modeled as shown in Figs. 5 and 4, respectively.

Displacement boundary conditions were required to constrain the model in order to get a unique solution. The column top and bottom nodes were restrained along the UX, UY and UZ directions in their respective planes to get the similarity of the experimental support conditions. The specimens were analyzed until it reached its maximum failure capacity when the program could not be converged. The finite element analysis of the model was set to analyze three different behaviors, that is, 1) initial cracking of the beam at the face of beam-column joint; 2) yielding of the steel reinforcement; and 3) behavior at the ultimate strength of the beam-column joint. In nonlinear analysis, the total load, divided into a series of load increments called load steps, was applied to the finite element model. At the completion of each incremental solution, the stiffness matrix of the model was adjusted to reflect nonlinear changes in stiffness using KUSE command before proceeding to the next load increment.

The ANSYS program uses the Newton–Raphson equilibrium iterations for updating the matrix of the model was adjusted to reflect nonlinear changes in stiffness using KUSE command before proceeding to the next load increment. In this study, for the reinforced concrete solid elements, convergence criteria were based on force and displacement, and the convergence tolerance limits were initially selected by the ANSYS program. It was found that convergence of solutions for the models was difficult to achieve due to the nonlinear behavior of reinforced concrete beam-column joints. Therefore, the convergence tolerance limits were increased to a maximum of 5 times the default tolerance limits (5% for force checking and 5% for displacement checking) in order to obtain convergence of the solutions.

The displacement and force convergence criteria were used for this analysis. These criteria were left at the default values before starting to crack the joint. However, when the column face (beam) began to crack, convergence for the nonlinear analysis was impossible with the default values and the displacements did not converge. Therefore, the value was multiplied by the tolerance during the nonlinear solution for convergence. A small criterion was used to capture correct response for the remainder of the analysis.

Table 6 Reinforcing bar diameter

	Reinforcing bar	Rebar dia
1	Column bar	12 mm
2	Beam bar	16 mm
3	Stirrup	6 mm
4	X-cross bar	12 mm

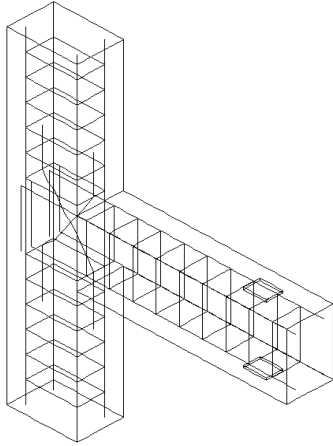


Fig. 4 Embedded reinforcing details

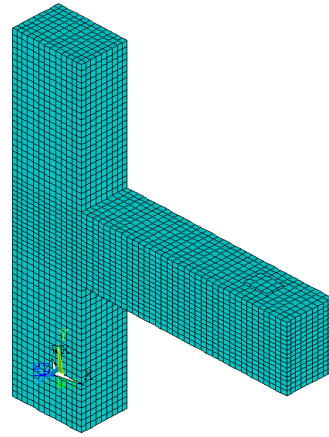


Fig. 5 Finite element discretization model

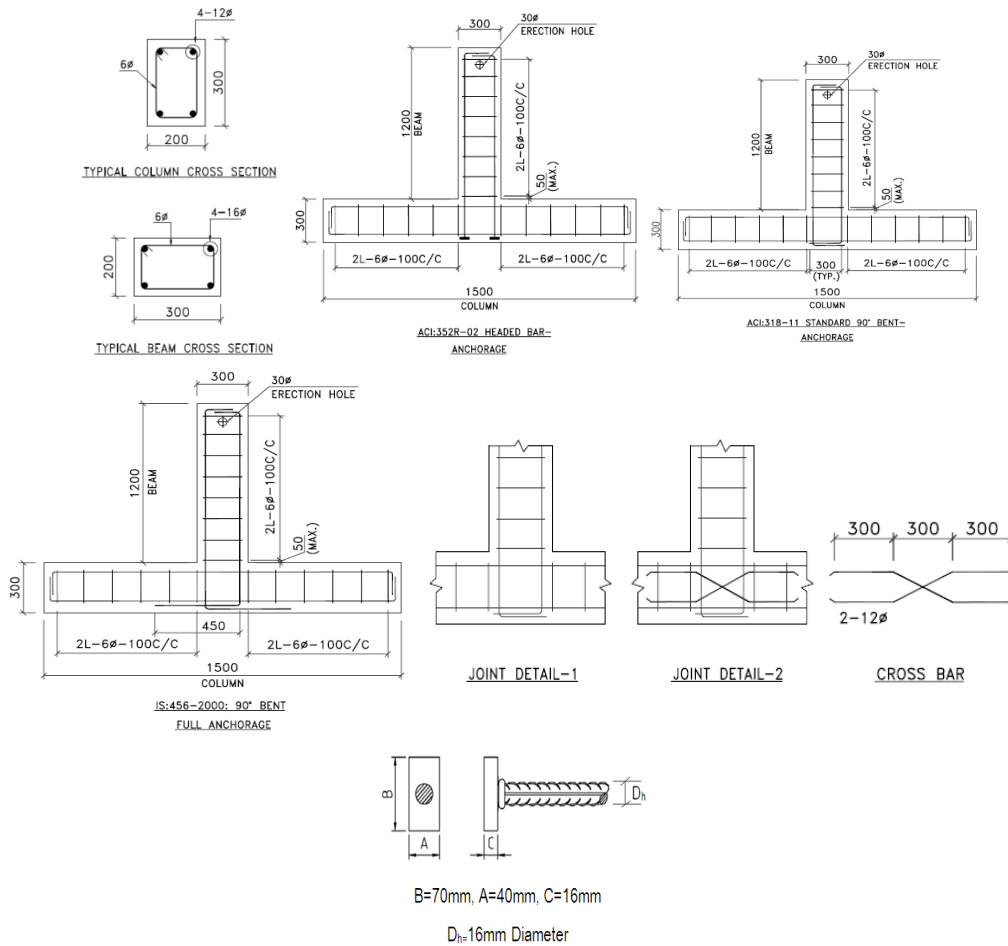


Fig. 6 Dimension and detailing of specimens (A1, A2, B1, B2, C1 and C2)

4. Summary of test specimens modeled and experimental set up

4.1 Test specimens modeled

The test and numerical analysis involves six numbers of specimens simulating the exterior beam-column joints as shown in Fig. 6. The specimens have been divided into two groups with and without X-cross bars (group-2 and group-1, respectively), each group having three specimens with different anchorages (heads, ACI 318 conventional hooks and IS 456 hooks with extended tails). The anchorage detailing of specimens A1 and A2 is T-type headed bars that followed ACI 352 (2002). The anchorage detailing of specimens B1 and B2 is standard conventional 90° bent hooks that followed ACI 318 (2011) and anchorage detailing of specimens C1 and C2 is 90° bent hooks with extended tails that followed IS 456 (2000). The group-1 specimens' joint details (A1, B1 and C1) have joint core details without shear ties, which are designed for the low seismic prone area as per IS 1893 (2002). The group-II specimens' joint details (A2, B2 and C2) have the proposed additional X-cross bars (Fig. 6). All the specimens of beam and column are of identical size. The beam size is 200 mm × 300 mm (width by depth). The column cross-section is 300 mm × 200 mm. The length of the beam is 1200 mm from the column face and the height of the column is 1500 mm. The various types of anchorages and joint details used are shown in Fig. 6, and the reinforcing bar diameters and anchorage details are indicated in Tables 6 and Fig. 6. Column, beam and joint reinforcing bar details and head details are also shown in Fig. 6. All the other experimental details are available elsewhere (Rajagopal and Prabavathy 2013).

4.2 Materials

Concrete mix was made with 43 Grade cement with river sand and 20 mm downgrade coarse aggregates. One cubic meter of concrete used for the test specimens contains cement of 435.45 kg, fine aggregates of 626.67 kg, coarse aggregates of 1188.22 kg, water of 191.6 kg with water/cement ratio of 0.45. The 28th day average cube compressive strength was 28.3 MPa. The reinforcing bars used were 6, 8, 12 and 16 mm diameter of grade Fe 415 and the grade of welded headed bars used was E410 (Fe 540).

4.3 Experimental set-up

The testing of half-scale exterior beam-column joint specimens was carried out at MEPCO Engineering College, Sivakasi, India. The joint assemblage was subjected to reversal loading using two hydraulic jacks of 25 ton capacity. The specimen column was kept in horizontal direction and beam was kept vertical. Both ends of the column were restrained in vertical and also in both horizontal directions by using strong built-up steel boxes which in turn were connected to the reaction floor using holding down anchor bolts. To facilitate application of reversal loading on either side of the beam, the hydraulic jacks were used which were connected to the strong steel frame with mechanical fasteners. The Linear Variable Differential Transducer (LVDT) was connected on either side of the specimen to monitor the displacement. The testing was load-controlled with a load increment of 1 ton. The specimen was tested until it reached its maximum failure capacity. Figs. 8 to 10 show hysteretic curves of load versus displacement relationship of all specimens that are modeled in this study.



Fig. 7 Experimental set-up

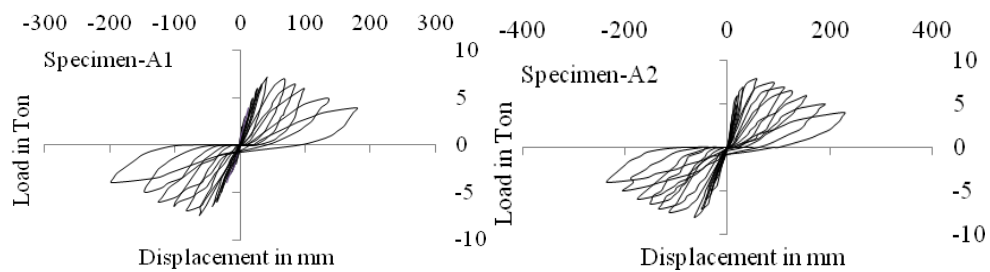


Fig. 8 Hysteretic curves of load versus displacement relationship for specimens A1 and A2

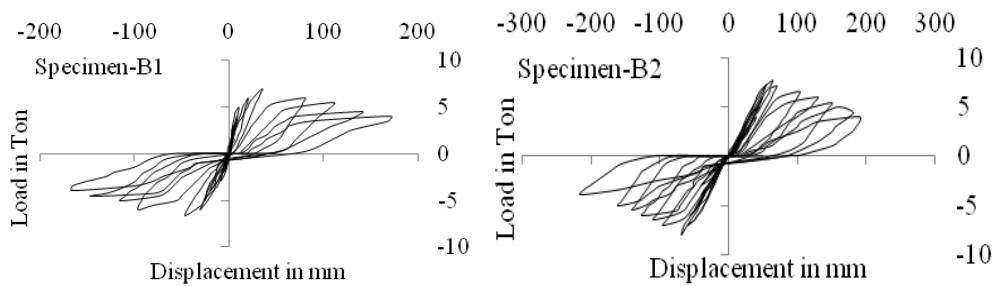


Fig. 9 Hysteretic curves of load versus displacement relationship for specimens B1 and B2

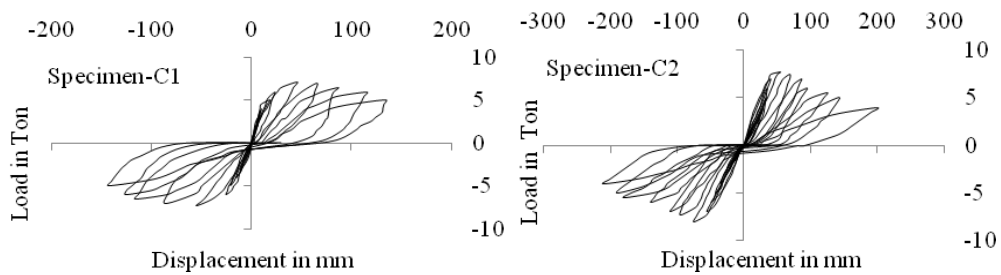


Fig. 10 Hysteretic curves of load versus displacement relationship for specimens C1 and C2

5. Nonlinear finite element analysis results

The load steps were taken to the initial cracking of the column face (beam). Once initial cracking was passed the load was increased until yielding of steel reinforcement occurred. After yielding of steel reinforcement, the load increment was reduced as the displacement began to increase more rapidly. Eventually, the load increment was further reduced to capture the failure of the joint. The failure of the beam-column joint occurred when the convergence failed due to deformation, and the corresponding load was the ultimate failure load in which the finite element analysis results are compared with test results.

5.1 Backbone curve of load versus displacement relationship

The backbone curves of the load versus displacement relationship for the experiment and finite element analysis are compared in Figs. 11 and 12 for specimens A1, B1 and C1 in group-I and A2, B2 and C2 in group-II, respectively, which were subjected to reversal lateral loading. It is observed that in group-I, the ultimate lateral load carrying capacities of the specimens A1, B1 and C1 were 73 kN, 68 kN and 71.75 kN with the corresponding lateral displacements of 52.7 mm, 40.9 mm and 50.6 mm, respectively. Among these, specimen A1 exhibited the maximum load carrying capacity. In group-II, the ultimate load carrying capacities of the specimens A2, B2 and C2 were 79.5 kN, 78.5 kN and 79.25 kN with the corresponding lateral displacements of 60.7 mm, 67 mm and 65.3 mm, respectively. For group-II, specimen A2 also exhibited the maximum lateral

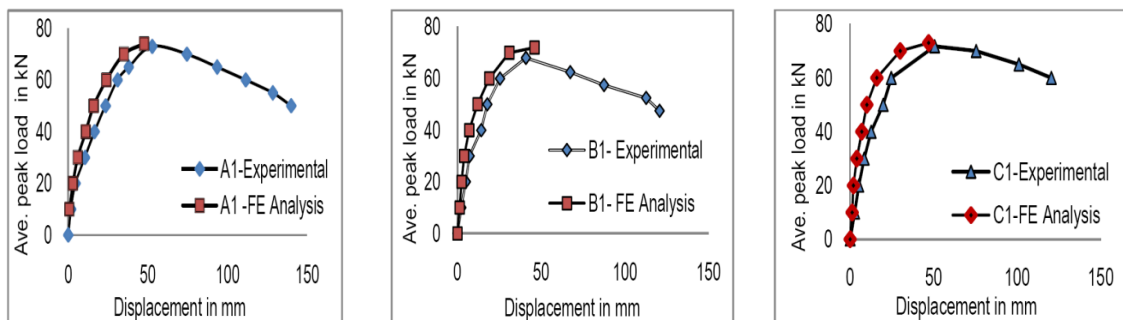


Fig. 11 Backbone curve of load versus displacement relationship of group-I specimens A1, B1 and C2

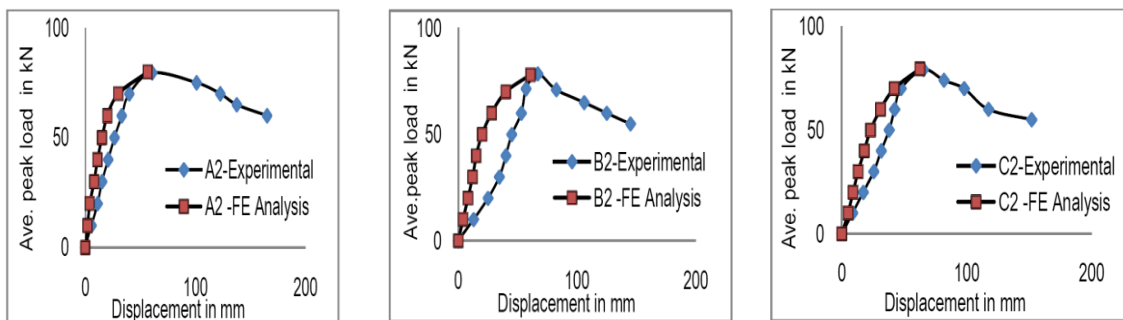


Fig. 12 Backbone curve of load versus displacement relationship of group-II specimens A2, B2 and C2

load carrying capacity over specimens B2 and C2. The results indicate that the anchorage behavior of headed bars is slightly better than that of hooked bars (with and without extended tails). It is also found that the extended tail of hooked bars improved the lateral load carrying capacity slightly. In terms of lateral ductility, similar results are found (Figs. 11 and 12).

The test results of load versus displacement relationship are validated using the ANSYS finite element analysis. The results of backbone curves of load versus displacement relationship are very close to those from the seismic tests as shown in Figs. 11 and 12 and as summarized in Table 12. It is seen from Figs. 11 and 12 that the specimens of group-II shows superior load carrying capacity (A2 by 8.2%, B2 by 13.4% and C2 by 9.5%) when compared to the specimens of group-I, indicating that the proposed additional X-cross bar increased the ultimate strength substantially.

5.2 Behavior from initial cracking to ultimate failure

The cracking pattern in the face of the column (beam junction) can be obtained using the Crack/Crushing plot option in ANSYS (2009). The initial cracking of the beam in the finite element model corresponds to a displacement that caused stress just beyond the modulus of rupture of the concrete (3.72 MPa). This first flexural crack occurred in the column face where the beam got connected.

5.2.1 Behavior at initial cracking

The cracking pattern in the face of the column (beam junction) can be obtained using the Crack/Crushing plot option in ANSYS (2009). The initial cracking of the beam in the finite element model corresponds to a displacement that caused stress just beyond the modulus of rupture of the concrete (3.72 MPa). This first flexural crack occurred in the column face where the beam got connected.

5.2.2 Behavior at ultimate failure

Yielding of steel reinforcement reached prior to or at maximum load and the displacements of the beam began to increase at a higher rate beyond this point. The capacity of the beam-column joint regained to distribute the load throughout the cross-section but soon diminished significantly due to the cracking of the concrete elements and yielding of steel reinforcing bars, which resulted in nonlinearity of concrete materials and reduced flexural rigidity of the members. Eventually, the greater deflection occurred at the beam edge due to these effects. The crack behavior is discussed in detail in the following paragraph.

Based on examination of crack patterns observed from both experimental and numerical analyses (Figs. 13 to 18), flexural cracks on the beam-column junction and shear cracks have developed on the column for all the specimens. Further to these cracks, 90° bent hooked bars of specimens B1, B2, C1 and C2 apparently induced a compressive stress in the joint diagonally forming a compression strut due to contact pressure under the bend. At the same time, it appeared that tension ties developed in the joint perpendicular to the direction of the strut, inducing a tensile stress. Diagonal cracks were developed perpendicular to the direction of the diagonal tension tie in the joint shear panel area. In addition to the wide open cracks in the junction, the concrete also crushed and spalled out for specimens B1, B2, C1 and C2 due to compressive force. Specimens A1 and A2 with headed bars, however, showed the lesser crack pattern than other specimens using conventional hooked bars both in group-I and group-II. Particularly, specimen A2 with both

headed bar anchorage and X-cross bars showed the least cracks and much better control of deterioration than other specimens. The X-cross bars were provided to control tensile failure in concrete of the joint shear panel area due to strut and tie action. Overall, it is found that the observed behavior is quite consistent between the experimental and numerical analyses. It can therefore be concluded that headed bar (mechanical) anchorage with the proposed joint core detailing of X-cross bars are much more effective in controlling the beam-column joint shear damage.

6. Conclusions

In this paper, nonlinear finite element analysis results on the reinforced concrete exterior beam-column joints with headed or hooked bars are compared with experimental results, and based on the comparison, the following conclusions are formulated.

1. Previous test results of the authors on the seismic behavior of exterior beam-column joints with headed or hooked bars were validated by nonlinear finite element analysis developed in this study. All the specimens showed very good agreements in terms of load versus displacement relationship and cracking patterns from initial cracking to its ultimate failure.

2. Among group-I and group-II specimens, the specimens with headed bars (mechanical anchorage) in accordance with ACI 352 had better seismic performance than the specimens with conventional 90° standard hooks in accordance with ACI 318 or IS 456.

3. Specimens in group-II (A2, B2 and C2) reinforced with X-cross bar detailing exhibited substantial improvement in degree of joint deterioration, strength and ductility than that of specimens in group-I. This is consistent with the simulated results using the ANSYS finite element analysis except for the ductility which was not numerically simulated in this study. The combination of headed bar anchorage and joint detailing of X-cross bars can be used for exterior beam-column joints assigned to Seismic Design Category A or B.

4. Both the experimental and analytical results proved that the use of headed bars (mechanical anchorage) is a viable alternative to the use of standard 90° hooks in exterior beam-column joints in regions of low to moderate seismicity. Mostly of all, headed bars effectively reduce the reinforcing congestion.

References

- ACI 318 (2011), *Building Code Requirements for Structural Concrete and Commentary*, American Concrete Institute, Farmington Hills, Michigan.
- ACI 352 (2002), *Recommendations for Design of Beam-Column Connections in Monolithic Reinforced Concrete Structures*, American Concrete Institute, Farmington Hills, Michigan.
- Al-Ta'an, S.A. and Ezzadeen, N.A. (1995), "Flexural analysis of reinforced fibrous concrete members using the FE method", *Comput. Struct.*, **56**(6), 1065- 1072.
- ANSYS (2009), *ANSYS Structural Analysis Guide*, Canonsburg, Pennsylvania.
- Ayoub, A. (2006), "Nonlinear analysis of reinforced concrete beam-columns with bond-slip", *ASCE J. Eng. Mech.*, **132**(11), 1177-1186.
- Baglin, P.S. and Scott, R.H. (2000), "Finite element modeling of reinforced concrete beam-column

- connection”, *ACI Struct. J.*, **97**(6), 886-894.
- Bindhu, K.R., Jaya, K.P. and Manicka Selvam, V.K. (2008), “Seismic resistance of exterior beam-column joints non-conventional reinforcement detailing”, *Struct. Eng. Mech.*, **30**(6), 733-761.
- Bindhu, K.R. and Jaya, K.P. (2010), “Strength and behaviour of exterior beam-column joints with diagonal cross bracing bars”, *Asian J. Civil Eng. (Building & Housing)*, **11**(3), 397-410.
- Chun, S.C., Lee, S.H., Kang, T.H.-K., Oh, B. and Wallace, J.W. (2007), “Mechanical anchorage in exterior beam-column joints subjected to cyclic loading”, *ACI Struct. J.*, **104**(1), 102-113.
- Dahmani, L., Khennane, S. and Kaci, S. (2010), “Crack identification in reinforced concrete beams using ANSYS”, *Strength Mater.*, **42**(2), 232-240.
- Hegger, J., Sherif, A. and Roeser, W. (2004), “Nonlinear finite element analysis of reinforced concrete beam-column connections”, *ACI Struct. J.*, **101**(5), 604-614.
- Ibrahim Ary, M. and Kang, T.H.-K. (2012), “Shear-strengthening of reinforced & prestressed concrete beams using FRP: part I – review of previous research”, *Int. J. Conc. Struct. Mater.*, **6**(1), 41-47.
- IS 456 (2000), *Plain and Reinforced Concrete - Code of Practice*, Bureau of Indian Standards, New Delhi, India.
- IS 1893 (2002), *Criteria for Earthquake Resistant Design of Structures - Part 1 : General Provisions and Buildings*, Bureau of Indian Standards, New Delhi, India.
- Kachlakev, D.I., Miller, T., Yim, S., Chansawat, K. and Potisuk, T. (2001), *Finite Element Modeling of Reinforced Concrete Structures Strengthened With FRP Laminates*, Research Report, Oregon Department of Transportation, Oregon.
- Kang, T.H.K., Ha, S.S. and Choi, D.U. (2010), “Bar pullout tests and seismic tests of small-headed bars in beam-column joints”, *ACI Struct. J.*, **107**(1), 32-42.
- Kang, T.H.-K., Howell, J., Kim, S. and Lee, D.J. (2012), “A state-of-the-art review on debonding failures of FRP laminates externally adhered to concrete”, *Int. J. Conc. Struct. Mater.*, **6**(2), 123-134.
- Kang, T.H.-K. and Mitra, N. (2012), “Prediction of performance of exterior beam-column connections with headed bars subject to load reversal”, *Eng. Struct.*, **41**, 209-217.
- Kang, T.H.-K., Shin, M., Mitra, N. and Bonacci, J.F. (2009), “Seismic design of reinforced concrete beam-column joints with headed bars”, *ACI Struct. J.*, **106**(6), 868-877.
- Kwak, H.G. and Filippou, F.C. (1997), “Nonlinear FE analysis of RC structures under monotonic loads”, *Comput. Struct.*, **65**(1), 1-16.
- Lam, K. M., Kim, W., Van Zandt, M. and Kang, T.H.-K. (2011), “An experimental study of reinforced concrete beams with closely-spaced headed bars”, *Int. J. Conc. Struct. Mater.*, **5**(2), 77-85.
- Li, B. and Kulkarni, S. (2010), “Seismic behavior of reinforced concrete exterior wide beam-column joints”, *ASCE J. Struct. Eng.*, **136**(1), 26-36.
- Park, S. and Mosalam, K.M. (2012), “Analytical model for predicting shear strength of unreinforced exterior beam-column joints”, *ACI Struct. J.*, **109**(2), 149-160.
- Rajagopal, S. and Prabavathy, S. (2013), “Study of exterior beam-column joint with different joint core and anchorage details under reversal loading”, *Struct. Eng. Mech.* in-press.
- Raongjant, W. and Jaig, M. (2008), “Finite element analysis on lightweight reinforced concrete shear wall with different web reinforcement”, *Proceedings of the 6th Prince of Songkla University Engineering Conference*, Songkhla, India, May.
- Shrestha, R., Smith, S.T. and Samali, B. (2013), “Finite element modeling of FRP-strengthened RC beam-column connections with ANSYS”, *Comput. Concr.*, **11**(1), 1-20.
- Tavarez, F.A. (2001), “Simulation of behavior of composite grid reinforced concrete beams using explicit finite element methods”, M.S. thesis, University of Wisconsin-Madison, Madison, Wisconsin.
- Willam, K.J. and Warnke, E.P. (1974), “Constitutive model for triaxial behaviour of concrete, Seminar on concrete structures subjected to triaxial stresses”, *Proceedings of International IABSE Conference on Concrete Structures Subject to Tri-Axial Stresses*, Bergamo, Italy.
- Wolanski, J.A. (2004), “Flexural behavior of reinforced and prestressed concrete beam using finite element analysis”, M.S. thesis, Marquette University, Milwaukee, Wisconsin.

- Xilin, L., Tonny, H.U., Sen, L. and Fangshu, L. (2012), "Seismic behavior of interior RC beam-column joints with additional bars under cyclic loading", *Earthq. Struct.*, **3**(1), 37-57.
- Xing, G.H., Wu, T., Niu, D.T. and Liu, X. (2013), "Seismic behavior of reinforced concrete interior beam-column joints with beams of different depths", *Earthq. Struct.*, **4**(4), 429-449.